Received: 13 September 2017 | Revised: 12 April 2018 | Accepted: 2 May 2018

DOI: 10.1002/fam.2638

RESEARCH ARTICLE

WILEY

Numerical study of polyethylene burning in counterflow: Effect of pyrolysis kinetics and composition of pyrolysis products

A. I. Karpov[1] | O. P. Korobeinichev[2] | A. A. Bolkisev[1] | A. A. Shaklein[1] | A. G. Shmakov[2,3] | A. A. Paletsky[2] | M. B. Gonchikzhapov[2,3]

[1] Udmurt Federal Research Center, Russian Academy of Science, Ural Branch, Institute of Mechanics, Izhevsk 426067, Russia

[2] Russian Academy of Science, Siberian Branch, Voevodsky Institute of Chemical Kinetics and Combustion, Novosibirsk 630090, Russia

[3] Novosibirsk State University, Novosibirsk 630090, Russia

Correspondence
A. I. Karpov, Institute of Mechanics, Udmurt Federal Research Center, Russian Academy of Science, Ural Branch, Izhevsk 426067, Russia.
Email: karpov@udman.ru

Funding information
Russian Science Foundation, Grant/Award Number: 16-49-02017

Summary

The burning behavior of polyethylene in the counterflow of oxidizing air has been studied numerically with a coupled model describing feedback heat and mass transfer between gas-phase flame and polymeric solid fuel. A 2-dimensional elliptic equation in axisymmetric formulation (revealing the cylindrical shape of the polymer sample used in the experiment) has been employed to simulate heat transfer in solid fuel, and a set of 1-dimensional hyperbolic equations has been used to determine the solid-to-gas conversion degree of the pyrolysis reaction. Four sets of products compositions and two modifications for the kinetic parameters of solid fuel pyrolysis reaction have been taken into account. Gas-phase formulation is presented by set of 1-dimensional conservation equations for multi-component flow with detailed kinetic mechanism of combustion. The profiles of temperature and species concentrations in the flame zone have been calculated and compared with the results of experimental study of combustion of ultrahigh molecular weight polyethylene. Higher hydrocarbon composition (dodecane) has been found to show the best agreement between the temperature and species concentration profiles with the measurements, especially for the low-level mass fractions of the by-product components—propylene, butadiene, and benzene.

KEYWORDS

counterflow combustion, numerical modeling, polyethylene burning, pyrolysis kinetics, pyrolysis products

1 | INTRODUCTION

Polymeric material behavior in fire is defined in general by mutually controlled gas-phase combustion and solid fuel pyrolysis. The chemical aspect of such an interaction relates to species composition of volatile products of polymer thermal degradation which are the gaseous fuel for combustion. Among the various polymers, there are ones (eg, polymethylmethacrylate) having a specific weak bond which destruction results in up to full content of monomer in degradation products. Unlike that case, for polymers such as polyethylene which has uniform chain structure, some oligomer formation is expected. In order to arrange the investigation of such a behavior, some typical experimental technique and configuration for modeling would be employed; the possible one is considered here.

The counterflow diffusion flame is primarily associated with gaseous oxidizer and fuel (see, for example, the survey paper[1]). To a large degree, such a configuration refers to the practical arrangement of combustion chambers, as well as provides a reasonable tool for investigation of the thermal and chemical processes taking place in model flames. Regarding the modeling of the counterflow flames, there are two crucial points which provide noticeable benefits and simplify the statement: in the physical sense, the flow is laminar, unless the off-design combustion regime occurs, and mathematically, set of governing equations is reduced to 1-dimensional formulation,

allowing to employ the widely used and well-approved numerical code OPPDIF.[2,3] Afterwards, the counterflow flame technique began to be applied[4-11] to combustion of solid fuels—polymers. However, the following substantially complicating factors arose from the viewpoint of modeling. Firstly, the "gas phase-solid fuel" interface becomes involved, being an input boundary for gaseous fuel species (polymer's pyrolysis products) consumed in the combustion reaction. Unlike in the gas flames, where the initial fuel temperature and the mass flow rate are arbitrarily prescribed (as for oxidizer), the surface temperature and the burning velocity of the solid fuel are not independent parameters but affected by the overall feedback interaction between gas-phase flame and solid fuel. Thus, the problem has to be considered by way of coupled analysis of the heat and mass transfer. Such a model was developed in T'ien et al,[12] where a second-order one-step overall chemical reaction was considered for gas-phase combustion. A detailed kinetic mechanism for modeling the diffusion flame of polyethylene was employed in [11] by using the OPPDIF code from the CHEMKIN software,[2,3] with uncoupled formulation considered: the surface temperature and the burning rate of solid fuel, as well as the composition of the pyrolysis products, were assigned through experimental data.[11] A coupled heat transfer model with complex combustion chemistry (using CHEMKIN) was presented in Yoshinaga and Kobayashi,[8] where a 1-dimensional equation was considered for the heat transfer in the solid fuel. This approach was applied to modeling of counterflow burning of polypropylene (later to the polyethylene[9]).

The most crucial issue concerning modeling of polymers burning (including the counterflow configuration) refers to the composition of gaseous pyrolysis products, which is the input parameter for the computational tool carrying out prediction of complex combustion chemistry and transport properties. Again, unlike in the case of gaseous reactants, we face the considerable degree of uncertainty in the information on the gases evaporating from the burning surface of the polymer. The simplest way (which also seems to be quite reasonable) to resolve this problem relates to assigning of monomer as a gaseous product of its polymer's thermal degradation. Such an approach was applied to polypropylene[8] and polyethylene.[9] However, even the fairly old data collected by the 1960s[13] showed that substantial amounts of up to C_7 hydrocarbons had been detected in the volatile products of pyrolysis of polyethylene considered here. With the further progress in the experimental technique, the presence of higher hydrocarbons up to C_{25} in the polyethylene pyrolysis products was reported.[10,11,14-17] Thus, the present study is focused on investigation of the effect of various compositions of polyethylene pyrolysis products on its burning behavior in counterflow. Along with this primary aim, the effect of pyrolysis kinetic parameters derived from the data achieved by different experimental techniques has been studied as well.

2 | FORMULATION

The experimental study of the combustion of ultrahigh molecular weight polyethylene in counterflow was carried out in Korobeinichev et al[10] and Gonchikzhapov et al.[11] A part of an apparatus containing a polymer sample is presented in Figure 1. To formulate the mathematical model, interpretation of such an arrangement has been accomplished as drawn in Figure 2.

The heat transfer behavior in the solid fuel is described by a 2-dimensional elliptic equation in axisymmetric formulation (revealing the polymer's cylindrical sample used in the experiment):

$$C_s\dot{m}\frac{\partial T_s}{\partial x} = \lambda_s\left(\frac{\partial^2 T_s}{\partial x^2} + \frac{1}{r}\frac{\partial}{\partial r}r\frac{\partial T_s}{\partial r}\right) + \rho_s W_s Q_s. \quad (1)$$

Here, C_s is the specific heat, $\dot{m}$ is the mass burning rate, T_s is the temperature, λ_s is the thermal conductivity, ρ_s is the density, and W_s and Q_s are the rate and heat of pyrolysis reaction, respectively.

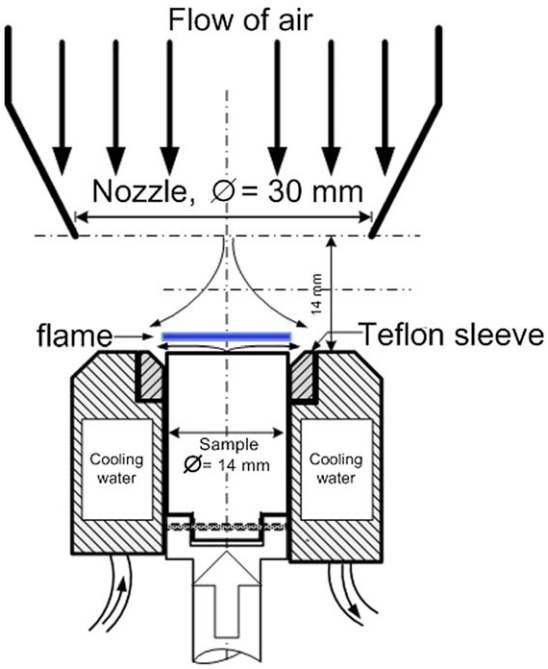

FIGURE 1 Sample arrangement in the experimental setup[10] [Colour figure can be viewed at wileyonlinelibrary.com]

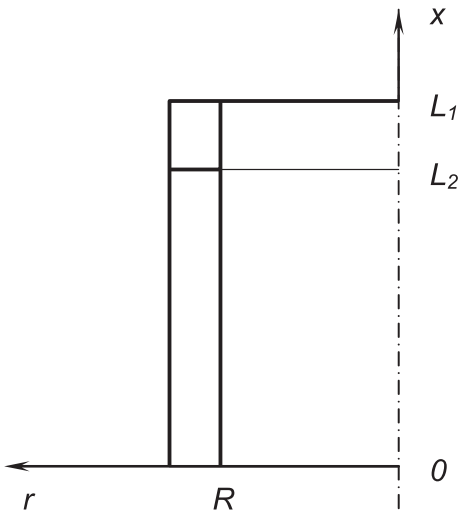

FIGURE 2 Computational domain

In the case of a non-zero order of pyrolysis reaction, the statement (1) is added by the set of 1-dimensional hyperbolic equations for "solid-to-gas" conversion

$$\dot{m}\frac{d\alpha}{dx} = \rho_s W_s, \tag{2}$$

where α is the conversion degree.

The boundary conditions correspondingly to the configuration of computational domain presented in Figure 2 are as follows:

$$x = 0,\ \ 0 \le r \le R:\ T_s = T_0,\ \ \alpha = 0, \tag{3}$$

$$r = R,\ \ 0 \le x \le L_2:\ T_s = T_0, \tag{4}$$

$$r = R,\ \ L_2 \le x \le L_1:\ \frac{\partial T_s}{\partial r} = 0, \tag{5}$$

$$r = 0,\ \ 0 \le x \le L_1:\ \frac{\partial T_s}{\partial r} = 0, \tag{6}$$

$$x = L_1,\ \ 0 \le r \le R:\ \lambda_s\frac{\partial T_s}{\partial x} + \dot{m}T_s(C_g - C_s) = q_g. \tag{7}$$

Here, Equation 3 represents the virgin solid fuel at the initial conditions, Equation 4 describes the interface between sample and recirculating water kept at constant temperature, Equation 5 corresponds to the sample's surface contacting with non-combustible teflon sleeve of low thermal conductivity, and Equation 6 is the symmetry axis condition. Equation 7 represents the coupled heat transfer at the burning surface, where q_g is the heat flux coming from the gas-phase flame.

The pyrolysis reaction's rate is determined as

$$W_s = k_s\varphi(\alpha)\exp\left(-\frac{E_s}{R_0 T_s}\right), \tag{8}$$

and integration of Equation 2 yields the mass burning rate of solid fuel

$$\dot{m} = \rho_s \int_0^{L_1} W_s dx. \tag{9}$$

Here, k_s is the preexponential factor, E_s is the activation energy, R_0 is the universal gas constant, and function $\varphi(\alpha)$ is approximated as

$$\varphi(\alpha) = (1-\alpha)^n(\alpha^m + \alpha_*), \tag{10}$$

where constants n, m, and α_* are defined below.

The gas-phase transport processes and chemical kinetics have been calculated by the Cantera open-source code[18] with the following 1-dimensional conservation equations for the steady-state axisymmetric stagnation flow:

$$\frac{d\rho u}{dx} + 2\rho V = 0, \tag{11}$$

$$\rho u\frac{dV}{dx} + \rho V^2 = -\Lambda + \frac{d}{dx}\left(\mu\frac{dV}{dx}\right), \tag{12}$$

$$\rho u C_p\frac{dT}{dx} = \frac{d}{dx}\left(\lambda\frac{dT}{dx}\right) - \sum_k C_{p,k}J_k\frac{dT}{dx} - \sum_k h_k M_k\dot{\omega}_k - \frac{dq^r}{dx}, \tag{13}$$

$$\rho u\frac{dY_k}{dx} = -\frac{dJ_k}{dx} + M_k\dot{\omega}_k. \tag{14}$$

Here, ρ is the density, u is the axial velocity, v is the radial velocity, $V = v/r$ is the scaled radial velocity, Λ is the pressure eigenvalue ($d\Lambda/dx = 0$), μ is the dynamic viscosity, C_p is the specific heat capacity at constant pressure, T is the temperature, λ is the thermal conductivity, Y_k, J_k, $C_{p,k}$, h_k, $M_k, \dot{\omega}_k$ are the mass fraction, diffusive mass flux, specific heat capacity, enthalpy, molecular weight, and the molar production rate of the k-th species, respectively, $dq^r/dx = 2\kappa_p\left(2\sigma T^4 - \varepsilon_s\sigma T_s^4 - \varepsilon_a\sigma T_a^4\right)$ is the radiative heat loss, T_s and T_a are the surface and ambient temperatures, respectively, ε_s and ε_a are emissivity values of surface and ambient gas, respectively, σ is the Stefan-Boltzmann constant, and κ_p is the Planck absorption coefficient.

Boundary conditions for the set of Equations 11 to 14 are to be assigned at the two points outlining the counterflow configuration: x_f for fuel input, which coincides with the solid fuel's burning surface ($x_f = L_1$ as shown in Figure 2) and x_a for the oxidizing gas flow. Thus, we have at x=xi:

$$\rho u = \dot{m}_i, \tag{15}$$

$$T = T_i, \tag{16}$$

$$J_k + \rho u Y_k = \dot{m}_f Y_{k,i}, \tag{17}$$

where $i = \{f, a\}$, $k = 1, N_i$, and N_f, N_a are the numbers of the initial species in fuel and oxidizing flows, respectively.

While for the latter case (x_a) the input parameters could be arbitrarily prescribed, the mass burning rate and temperature on the burning surface are determined through the solution of Equations 1 to 9, and concentrations of gaseous fuel are assigned using certain premises for the composition of pyrolysis products. In turn, the solution of gas-phase equations 11 to 14 provides the heat flux from the flame zone to the solid fuel surface

$$q_g = \lambda\frac{dT}{dx} + \frac{1}{2}\int_{x_f}^{x_a}\frac{dq^r}{dx}dx, \tag{18}$$

which is set as a boundary condition (7) for prediction of heat transfer in the solid fuel. Such an iteration procedure was successively carried out until a convergent solution was obtained.

Equations 11 to 14 were filled with the data for the species' transport properties[19] and with a detailed kinetic mechanism for combustion reactions.[20,21]

3 | INPUT DATA

Table 1 presents two sets of kinetic parameters of pyrolysis reaction considered here, which were derived from the measurements in counterflow flame[22] and by microscale combustion calorimetry.[23]

Another point is to be taken into account to finalize the physical content of the presented mathematical model. As found in the experimental study,[10] the process of thermal degradation of ultrahigh molecular-weight polyethylene results in formation of a melted layer on the burning surface. Thereafter, liquid products drip from the sample's surface and thus were not involved in the gas-phase

TABLE 1 Kinetic parameters of the pyrolysis reaction

No.	Ref.	k_s, 1/s	E_s, kJ/mole	Constants in Equation 10		
				n	m	α_*
1	[22]	$2.29 \cdot 10^8$	143	$\varphi(\alpha) = 1$		
2	[23]	$1.08 \cdot 10^{13}$	211.8	0.82	0.68	0.03

combustion reaction. The mass fraction of the volatile pyrolysis products was evaluated as being approximately 70%. Therefore, the relationship (9) for fuel's mass burning rate was corrected for its actual value, which stands for the boundary condition (15):

$$\dot{m}_f = \gamma \dot{m}. \tag{19}$$

Here, $\gamma \simeq 0.7$. Following this consideration, the heat consumption in Equation 1 is estimated as $Q_s = Q_m + \gamma Q_d$, where $Q_m =$ - 218kJ/kg is the heat of melting and $Q_d =$ - 920kJ/kg is the heat of decomposition (gasification),[24] which results in the $Q_s =$ - 862kJ/kg.

The physical properties of polyethylene are $C_s = 1.41 + 0.00896T$ J/(g·°C) for $T < T_m$ and $C_s = 1.76 + 0.00508T$ J/(g·°C) for $T > T_m$, where $T_m = 134^{\circ}C$ is the melting temperature,[24] $\lambda_s = 0.44$W/(m·K), $\rho_s = 920$kg/m^3,[22] and the sample sizes (Figure 2) are[22]: radius is $R = 7$mm, length is $L_1 = 40$mm, and teflon sleeve thickness is $(L_1 - L_2) = 3$mm. The air flow mass fractions are[22] $Y_{O_2} = 0.233$ and $Y_{N_2} = 0.767$, and mass velocity is $\dot{m}_a = (\rho u)_a = 0.54$kg/(m^2·s), the distance between the solid fuel surface and the air flow nozzle is[10] $(x_a - x_f) = 14$mm, and the initial temperature is $T_0 = 300$K.

In accordance with the primary aim of the present study pointed out earlier, several compositions of the pyrolysis products are taken into account, which are listed in Table 2.

For the modeling of detailed chemical kinetics of gas-phase combustion, two mechanisms were employed: 1997 reactions and 300 species for scheme involving lower hydrocarbons C_1–C_4[20] and 1411 reactions and 163 species for higher hydrocarbons up to C_{12}.[21]

The averaged Planck absorption coefficient is $\kappa_p = \sum_i \kappa_{p,\,i}(T) X_i$, where $\kappa_{p,\,i}$ is the individual value of Planck absorption coefficient determined from Hongmei and Modest[25] and Wakatsuki et al[26] and X_i is the mole fraction of i-th species. The optical thickness is defined as[27] $\tau = \int_{x_f}^{x_a} \kappa_p dx$, and assumption of optically thin layer requests the condition $\tau \ll 1$. Test run of calculations has been carried out showing that value of τ has an order of 0.009, ensuring the optically thin layer is acceptable.

TABLE 2 Compositions of gaseous pyrolysis products

No.	Composition of Pyrolysis Products		Ref.	Pyrolysis Reaction, Table 1	Combustion Mechanism Ref.
	Species	Mass fraction			
1	C_2H_4 C_2H_6 C_3H_6 C_3H_8 C_4H_6 C_4H_8 C_4H_{10}	0.03 0.097 0.056 0.168 0.004 0.357 0.287	[13]	1	[20]
2	C_3H_6 C_4H_6 C_6H_6	0.28 0.57 0.15	[11]	1	[20]
3	$C_{12}H_{26}$	1.0		1	[21]
4	$C_{12}H_{26}$	1.0		2	[21]
5	C_2H_4	1.0	[9]	1	[20]

4 | RESULTS AND DISCUSSION

Firstly, the argumentation has to be outlined to back the mathematical model formulated above. Our previous experimental studies[28,29] of counterflow flame have been indented (along with primary aims) specifically to evaluation of the effect of thermocouple and species sampling probe position in gas phase relatively to the symmetry axis of configuration shown in Figures 1 and 2. These results have shown that temperature and species profiles measured at the axis and at the periphery as far as 5 mm from the axis (note the sample radius is 7 mm for the case considered here) are close enough to conclude the 1-dimensional flame occurs definitely. Unlike the gas-phase parameters, solid fuel temperature is substantially affected by the specific arrangement of experimental setup (Figures 1 and 2). Boundary condition on the outer side of polymer sample is determined by different thermal regimes: permanent cooling defined by Equation 4 and adiabatic condition expressed by Equation 5. Such an effect has been analyzed in Appendix.

Figure 3 presents the temperature profiles in the flame zone calculated by using the compositions of various pyrolysis products as indicated in Table 2. Here, the coordinate $x = 0$ corresponds to burning surface. It can be noted that for the first choice of pyrolysis kinetics (Table 1), an increase of molecular weight of pyrolysis products results in the smaller flame temperature gradually approaching the experimental values. Such a tendency may be explained generally by the endothermic effect of the thermal decomposition of higher hydrocarbons occurring in the zone adjacent to the burning surface. However, even the best numerical result achieved for dodecane (curve 3) overestimates the experimental temperature. As for the case of ethylene (curve 5), the temperature exceeds noticeably the measurements data and reaches the level of 2000 K, close to the calculations,[9] where a monomer was assigned as a possible product of polyethylene pyrolysis.

For the second set of pyrolysis kinetic parameters, almost perfect agreement with the experimental temperature was achieved (curve 4) if dodecane was used as a pyrolysis product.

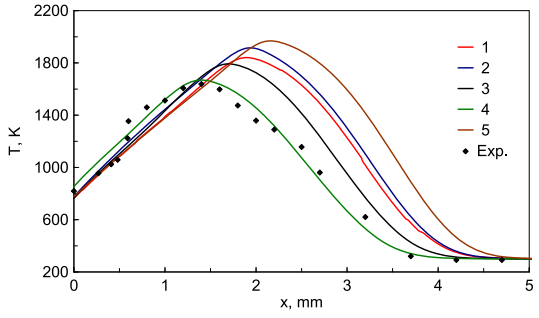

FIGURE 3 Temperature distribution in flame; symbols—experiment[10,11]; curves—calculations, number of case is indicated in Table 2 [Colour figure can be viewed at wileyonlinelibrary.com]

Figures 4–8 present the species profiles in the flame zone. Here, the coordinate $x = 0$ corresponds to burning surface, graphs (A) and (B) are drawn in different scales for different species and nitrogen is scaled out because its calculated profile perfectly fits the experimental data for all the cases considered. Overall analysis of the concentration profiles of low-molecular gases (carbon monoxide, carbon dioxide, water vapor, and oxygen presented in graphs (A)) showed that more or less reasonable qualitative agreement with the experimental data

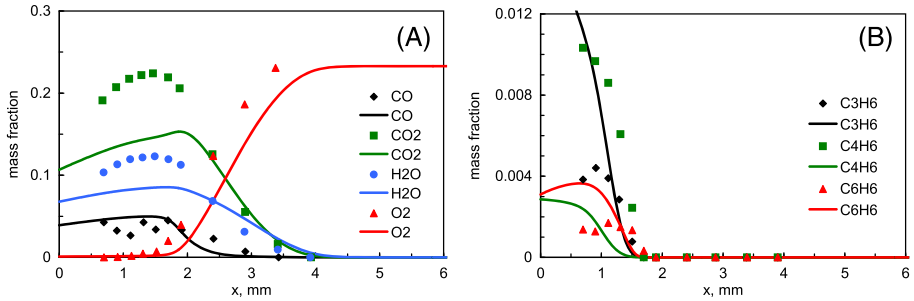

FIGURE 4 Species concentration profiles in flame for case 1 (Table 2); symbols—experiment[10]; curves—calculations [Colour figure can be viewed at wileyonlinelibrary.com]

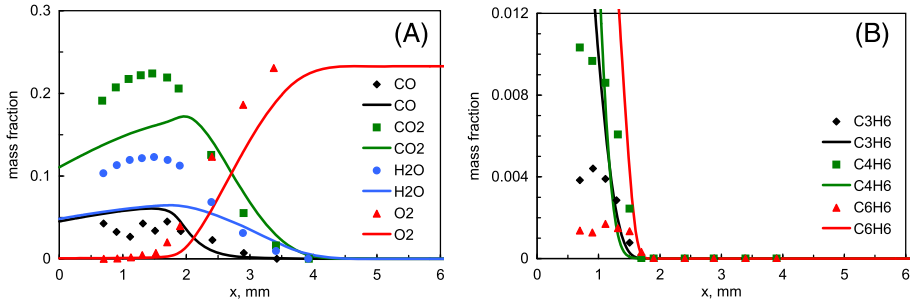

FIGURE 5 Species concentration profiles in flame for case 2 (Table 2); symbols—experiment[10]; curves—calculations [Colour figure can be viewed at wileyonlinelibrary.com]

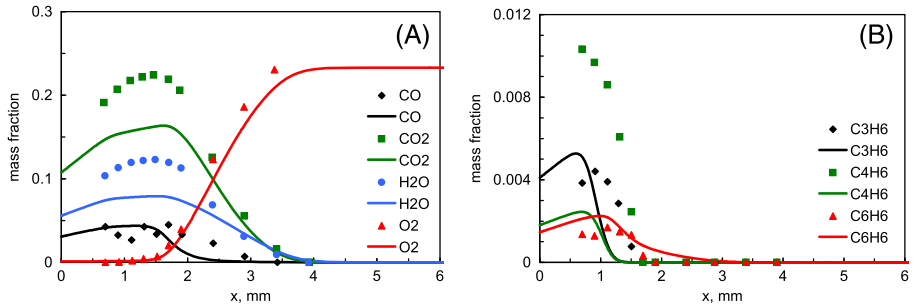

FIGURE 6 Species concentration profiles in flame for case 3 (Table 2); symbols—experiment[10]; curves—calculations [Colour figure can be viewed at wileyonlinelibrary.com]

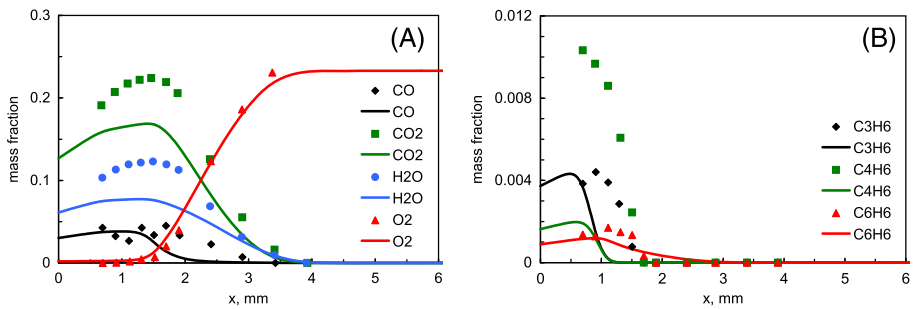

FIGURE 7 Species concentration profiles in flame for case 4 (Table 2); symbols—experiment[10]; curves—calculations [Colour figure can be viewed at wileyonlinelibrary.com]

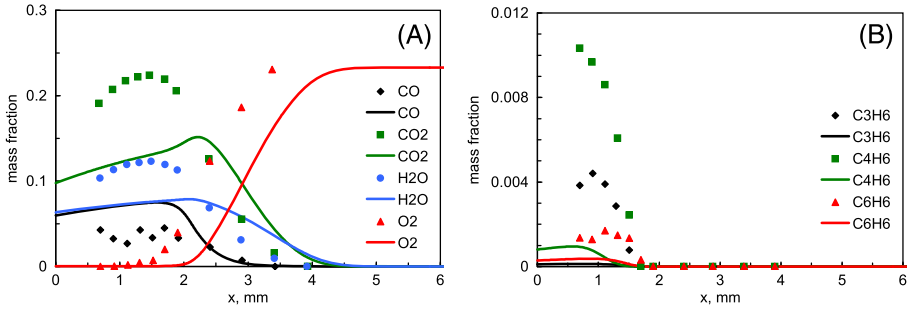

FIGURE 8 Species concentration profiles in flame for case 5 (Table 2); symbols—experiment[10]; curves—calculations [Colour figure can be viewed at wileyonlinelibrary.com]

has been obtained. Again, as it has been found for the temperature profile, the presence of a higher hydrocarbon (dodecane) in the pyrolysis products (Figures 6 and 7) provides a better quantitative agreement, while low-weight ethylene (Figure 8) shows the poorest one.

The concentration profiles of low-level mass fractions of some hydrocarbons (propylene, butadiene, and benzene shown in graph (B) of Figures 4–8), which have been measured in experiment,[10,11] provide a fairly interesting background for the analysis. The composition for the case 1 corresponds to pyrolysis at a low heating rate and without oxidation. Calculations for this composition containing C_3H_6 and C_4H_6 in pyrolysis products showed (Figure 4B) C_4H_6 to be underestimated, while C_3H_6 dropped from the assigned mass fraction 0.05 at the burning surface (Table 2) to the reasonable values in the flame zone. Although there were no hydrocarbons higher than C_4 among the pyrolysis products, C_6H_6 is formed and its mass fraction is overestimated almost twice, compared with the experimental data.

The composition of the pyrolysis products for case 2 was based on the results of experimental studies[10,11] where propylene, butadiene, and benzene were identified in the counterflow flame of ultrahigh molecular weight polyethylene. It has to be noted that the nearest point of measurements was at the distance of 0.8 mm away from the burning surface. Transferring this composition to the burning surface, a model (C_3H_6 + C_4H_6 + C_6H_6)/air flame was investigated numerically in our previous study[11] by the uncoupled approach, where heat transfer in the solid phase was not considered. Because the boundary conditions for the fuel input (temperature and mass burning rate at the polymer's surface) were assigned using the experimental data, a good agreement of the temperature profile with experiment was achieved in Gonchikzhapov et al.[11] In the present calculations, based on the coupled analysis where surface temperature was not strictly appointed but determined through the joint solution of gas-phase and solid fuel conservation equations, the discrepancy in temperature distributions was found (curve 2 in Figure 3). As for the species concentrations (Figure 5A), the present calculations showed the concentration profiles which behavior is very similar to Gonchikzhapov et al[11]: CO and O_2 were predicted rather acceptably while CO_2 and H_2O are underestimated. Figure 5B presents the mass fractions of the species taken here as possible pyrolysis products. The near-surface values of C_3H_6, C_4H_6, and C_6H_6 mass fractions significantly exceeded the experimental points, the fact being quite expected due to the previously mentioned assumption consisting in the arbitrary transfer of the measured values from the flame zone to the burning surface to the 0.8-mm distance. At the same time, along the distance, the calculated values of the propylene, butadiene, and benzene concentrations approached the experimental data and adequately disappeared in the flame zone just before 2 mm from the burning surface.

The composition of the pyrolysis products for the case 3 was derived from the following reasoning: as pointed out earlier, the hydrocarbons up to C_{25} were identified in the polyethylene pyrolysis products,[10,11,14-17] and the C/H ratio was established[10] on the level of 85% for the carbon mass fraction. Thus, dodecane fits the latter conclusion and may represent some averaging result for the former one. The calculated mass fractions presented in Figure 6A show that better agreement has been achieved than for the cases 1 and 2, especially for O_2 and CO concentration profiles. As for the data shown in Figure 6B, C_3H_6 and C_6H_6 concentration profiles were predicted quite well, while C_4H_6 was underestimated. Then, dodecane was assigned as a pyrolysis product for case 4, where the second set of kinetic parameters of the pyrolysis reaction was employed. The profiles of the mass fractions presented in Figure 7 show a behavior which is very similar to the previous case (Figure 6), but all curves have moved slightly from the flame zone towards the burning surface.

As pointed out earlier, the results for the case 5, where C_2H_4 is assumed to be a pyrolysis product, showed the poorest agreement with experimental data, both for temperature (curve 5 in Figure 3) and mass fractions (Figure 8). Nevertheless, some interesting effect followed from the Figure 8B: even if the pure ethylene is the only input gaseous fuel, higher hydrocarbons such the propylene, butadiene, and benzene are predicted in the combustion reaction zone.

Table 3 presents summarized numerical results. The case number in Table 3 corresponds to the case number in Table 2. Along with the explicit values of flame and surface temperatures, the concentration profiles of which are shown in Figure 3, the mass burning rate of solid fuel has been evaluated. This macroscopic parameter (calculated from Equation (9)) has to be considered as a very important factor expressing the overall effect of feedback interaction between gas-phase combustion and solid fuel pyrolysis. It can be noticed that calculations using pyrolysis kinetics derived from the counterflow flame conditions[22] provide a reasonable agreement with the experimental data on the mass burning rate. As for the kinetic parameters obtained by microscale combustion calorimetry,[23] the mass burning rate was found to be substantially underestimated, because such a content is hardly applicable to the polymer's sample mass of approximately

TABLE 3 Solid fuel and gas-phase summary parameters

No.	Mass Burning Rate, g/(s·m^2)	Surface Temperature, K	Maximum Flame Temperature, K	Surface Heat Flux, kW/m^2	
				Conductive	Radiant
Exp.[10]	14.4	823	1638	n/a	n/a
1	13.2	768	1841	46.8	3.4
2	16.4	777	1915	52.9	4.6
3	13.3	765	1792	45.8	3.0
4	7.5	854	1669	48.7	2.8
5	16.3	776	1968	50.6	5.2

3 mg. Moreover, the heating rate of around 1 K/s carried out here stands rather far from that realized in counterflow combustion. The data presented in Table 3 showed the contribution of surface radiative heat flux to be of the level less than 10% for all investigated cases.

5 | CONCLUDING REMARKS

The numerical study of polyethylene burning in counterflow has been carried out with primary focus on the effect of the composition and kinetics of the pyrolysis products. Various sets of polyethylene pyrolysis products and kinetic parameters have been investigated. It has been found that higher hydrocarbon, namely, dodecane, showed good agreement with the experimental data on the species concentration, as shown in Figures 6 and 7. Along with the proper distributions of ordinary (fuel-oxidizer-product) species taking part in a general combustion reaction (graphs (A) in Figures 6 and 7), the most remarkable result follows from the graphs (B) of these figures. Unlike in cases 1 and 2, where propylene and butadiene are someway included into the polyethylene pyrolysis products, the reacting behavior of dodecane in the flame showed the independent generation of propylene, butadiene, and benzene. Being the by-products of combustion reaction, these components are not necessarily analyzed in the flame structure, and this result actually confirms the reasonability of choosing higher hydrocarbons for the possible pyrolysis product of polyethylene. Following the results of the experimental study of polyethylene pyrolysis,[10,11,14-17] where products up to C_{25} were identified, the hopeful direction of further investigation relates to employing the reaction kinetic schemes taking into account higher hydrocarbons and increasing the variety of species (eg, Sukumaran and Kong[30]).

ACKNOWLEDGEMENT

This work was supported by the Russian Science Foundation (Project 16-49-02017).

ORCID

A. I. Karpov http://orcid.org/0000-0001-8380-1599

REFERENCES

1. Tsuji H. Counterflow diffusion flames. *Prog Energy Combust Sci*. 1982;8(2):93-119. https://doi.org/10.1016/0360-1285(82)90015-6
2. Lutz AE, Kee RJ, Grcar JF, Rupley FM. OPPDIF: a Fortran program for computing opposed-flow diffusion flames. *Sandia National Laboratories Report*. 1996;96-8243.
3. Kee RJ, Rupley FM, Miller JA, et al. *CHEMKIN Collection, Release 3.6*. San Diego, CA: Reaction Design, Inc.; 2000.
4. Richard JR, Vovelle C, Delbourgo R. Flammability and combustion properties of polyolefinic materials. *Proc Combust Inst*. 1975;15(1):205-216. https://doi.org/10.1016/S0082-0784(75)80298-0
5. Holve DJ, Sawyer RF. Diffusion controlled combustion of polymers. *Proc Combust Inst*. 1975;15(1):351-361. https://doi.org/10.1016/S0082-0784(75)80310-9
6. Seshadri K, Williams FA. Structure and extinction of counterflow diffusion flames above condensed fuels: comparison between poly(methyl methacrylate) and its liquid monomer, both burning in nitrogen-air mixtures. *J Polym Sci A Polym Chem*. 1978;16(7):1755-1778. https://doi.org/10.1002/pol.1978.170160726
7. Pitz WJ, Brown NJ, Sawyer RF. The structure of a poly(ethylene) opposed flow diffusion flame. *Proc Combust Inst*. 1981;18(1):1871-1879. https://doi.org/10.1016/S0082-0784(81)80193-2
8. Yoshinaga K, Kobayashi H. Numerical study of radiation effects on polypropylene combustion using high-temperature oxidizer diluted with H_2O and CO_2. *Journal of Thermal Science and Technology*. 2008;3(2):167-178. https://doi.org/10.1299/jtst.3.167
9. Ogami Y, Mori M, Yoshinaga K, Kobayashi H. Experimental study on polymer pyrolysis in high-temperature air diluted by H_2O and CO_2 using stagnation-point flow. *Combust Sci Technol*. 2012;184(6):735-749. https://doi.org/10.1080/00102202.2012.661496
10. Korobeinichev OP, Gonchikzhapov MB, Paletsky AA, et al. Counterflow flames of ultrahigh-molecular-weight polyethylene with and without triphenylphosphate. *Combust Flame*. 2016;169:261-271. https://doi.org/10.1016/j.combustflame.2016.04.019
11. Gonchikzhapov MB, Paletsky AA, Tereshchenko AG, et al. Structure of ultrahigh molecular weight polyethylene-air counterflow flame. *Combustion, Explosion, and Shock Waves*. 2016;52(3):260-272. https://doi.org/10.1134/S0010508216030023
12. T'ien JS, Singhal SN, Harrold DP, Prahl JM. Combustion and extinction in the stagnation-point boundary layer of a condensed fuel. *Combust Flame*. 1978;33:55-68. https://doi.org/10.1016/0010-2180(78)90045-7
13. Madorsky SL. *Thermal Degradation of Organic Polymers*. New York: Interscience Publ; 1964:315.
14. Onwudili JA, Insura N, Williams PT. Composition of products from the pyrolysis of polyethylene and polystyrene in a closed batch reactor: effects of temperature and residence time. *J Anal Appl Pyrolysis*. 2009;86(2):293-303. https://doi.org/10.1016/j.jaap.2009.07.008
15. Gascoin N, Fau G, Gillard P, Mangeot A. Experimental flash pyrolysis of high density polyethylene under hybrid propulsion conditions. *J Anal Appl Pyrolysis*. 2013;101:45-52. https://doi.org/10.1016/j.jaap.2013.02.014
16. Faravelli T, Bozzano G, Scassa C, et al. Gas product distribution from polyethylene pyrolysis. *J Anal Appl Pyrolysis*. 1999;52(1):87-103. https://doi.org/10.1016/S0165-2370(99)00032-7

17. Bruns MC, Ezekoye OA. Modeling differential scanning calorimetry of thermally degrading thermoplastics. *J Anal Appl Pyrolysis*. 2014;105:241-251. https://doi.org/10.1016/j.jaap.2013.11.010
18. Goodwin DG, Moffat HK, Speth RL. Cantera: An object-oriented software toolkit for chemical kinetics, thermodynamics, and transport processes, Version 2.2.1. http://www.cantera.org Accessed April 11, 2018
19. McBride BJ, Gordon S, Reno MA. Coefficients for calculating thermodynamic and transport properties of individual species. *NASA Tech Memo*. 1993;4513.
20. Wang H, You X, Joshi V, Davis S, Laskin A, Egolfopoulos F, Law C. USC Mech Version II. high-temperature combustion reaction model of H_2/CO/C_1-C_4 compounds, 2007. http://ignis.usc.edu/USC_Mech_II.htm Accessed April 11, 2018
21. Pei Y, Mehl M, Liu W, Lu T, Pitz WJ, Som S. A multi-component blend as a diesel fuel surrogate for compression ignition engine applications. Journal of Engineering for Gas Turbines and Power GTP-15-1057, 2015. https://combustion.llnl.gov/mechanisms/surrogates/diesel-surrogate-detailed-and-reduced Accessed April 11, 2018
22. Korobeinichev OP, Gonchikzhapov MB, Paletsky AA, et al. Study of counterflow flame of ultrahigh-molecular-weight polyethylene with and without triphenylphosphate. Proceedings of the Eighth International Seminar on Fire and Explosion Hazards, University of Science and Technology of China, Hefei, 2016;465–475. https://doi.org/10.20285/c.sklfs.8thISFEH.048
23. Snegirev AY, Talalov VA, Stepanov VV, Korobeinichev OP, Gerasimov IE, Shmakov AG. Autocatalysis in thermal decomposition of polymers. *Polym Degrad Stab*. 2017;137:151-161. https://doi.org/10.1016/j.polymdegradstab.2017.01.008
24. Stoliarov SI, Walters RN. Determination of the heats of gasification of polymers using differential scanning calorimetry. *Polym Degrad Stab*. 2008;93(2):422-427. https://doi.org/10.1016/j.polymdegradstab.2007.11.022
25. Hongmei Z, Modest MF. Evaluation of the Planck-mean absorption coefficients from HITRAN and HITEMP databases. *J Quant Spectrosc Radiat Transfer*. 2002;73:649-653.
26. Wakatsuki K, Jackson GS, Kim J, Hamins A, Nyden MR, Fuss SP. Determination of Planck mean absorption coefficients for hydrocarbon fuels. *Combust Sci Technol*. 2008;180(4):616-630. https://doi.org/10.1080/00102200701838941
27. Sparrow EM, Cess RD. *Radiation Heat Transfer*. Belmont, CA: Brooks Pub; 1966:322.
28. Knyazkov DA, Shmakov AG, Korobeinichev OP. Application of molecular beam mass spectrometry in studying the structure of a diffusive counterflow flame of CH_4/N_2 and O_2/N_2 doped with trimethylphosphate. *Combust Flame*. 2007;151(1-2):37-45. https://doi.org/10.1016/j.combustflame.2007.06.011
29. Korobeinichev OP, Gonchikzhapov MB, Paletsky AA, et al. Structure of counterflow flame of ultrahigh-molecular-weight polyethylene with and without triphenylphosphate. *Proc Combust Inst*. 2017;36(2):3279-3286. https://doi.org/10.1016/j.proci.2016.06.117
30. Sukumaran S, Kong SC. Modelling biodiesel-diesel spray combustion using multicomponent vaporization coupled with detailed fuel chemistry and soot models. *Combust Theor Model*. 2016;20(5):913-940. https://doi.org/10.1080/13647830.2016.1199917

How to cite this article: Karpov AI, Korobeinichev OP, Bolkisev AA, et al. Numerical study of polyethylene burning in counterflow: Effect of pyrolysis kinetics and composition of pyrolysis products. *Fire and Materials*. 2018;1–8. https://doi.org/10.1002/fam.2638

APPENDIX

In order to estimate the effect of specific arrangement of experimental setup shown in Figure 1, 1-dimensional analysis has been carried out. Thus, solid fuel energy Equation (1) is reduced to

$$C_s \dot{m} \frac{\partial T_s}{\partial x} = \lambda_s \frac{\partial^2 T_s}{\partial x^2} + \rho_s W_s Q_s, \tag{A1}$$

with the same boundary conditions (3) and (7). Such a formulation[8] is rather expected in a view to correspond fully to 1-dimensional conservation equations employed for gas phase. However, unlike the actual experimental conditions, 1-dimensional model does not take into account neither cooling of sample's outward side nor its cylindrical shape.

Figure A1 presents the temperature distribution in solid fuel. Case 3 (Table 2) is shown here, while the other cases have actually the same behavior. It is obvious that the effect of sample's side cooling and the thickness of adiabatic teflon sleeve is significant. The most remarkable quantitative effect consists in following: due to increased heating depth, the 1-dimensional model predicts the value of mass burning rate 29.3 g/(s·m^2), which is twice higher than experimental result as indicated in Table 3.

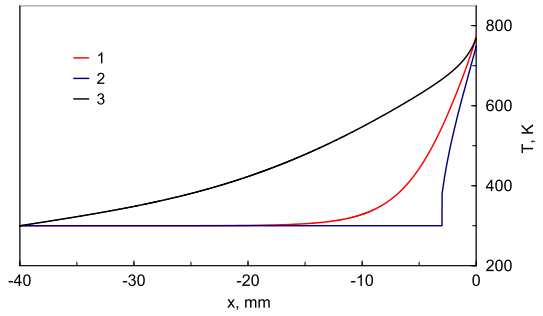

FIGURE A1 Temperature distribution in solid fuel; 1—axis (r = 0), 2—side (r = R), 3—1-dimensional [Colour figure can be viewed at wileyonlinelibrary.com]